The Effects of Preheating the Shielding Gas Used in Gas Tungsten Arc Welding

A methodology for studying the electric arc was proposed, evaluating the voltage-current, profile, and luminosity values

BY N. NOGUEIRA DA SILVA AND W. SADE

Abstract

The shielding gas used in welding processes has properties that can affect the operating characteristics of electric welding arcs. Characteristics such as welding voltage, heat input, and thermal profile, which in turn affect weld geometry, are strongly influenced by the properties of the gas used. Thus, this work aimed to evaluate how preheating the shielding gas influences the gas tungsten arc welding (GTAW) process. For this, a heating system was developed that allowed the variation and control of the gas exit temperature during the tests. A methodology for studying the electric arc was proposed, evaluating the voltage-current, profile, and luminosity values. Autogenous welds were performed on carbon steel plates with different gas temperatures, and penetration and width were observed. The results showed that the use of gas preheating influenced the characteristics of the arc and, consequently, weld geometry.

Keywords

- Welding Physics
- Gas Tungsten Arc Welding
- Properties of Shielding Gas
- Welding Gas Heating

Introduction

The electric arc is the heat source most used in the fusion welding of metallic materials as it has an optimal combination of characteristics, including an adequate concentration of energy for localized fusion of the base metal. Therefore, the processes in which the electric arc is used are of great industrial importance because it is used in the manufacture of the most varied components and metallic structures and the recovery of damaged or worn parts (Refs. 1, 2).

A process that makes use of the electric arc as a source of energy for the fusion of the materials to be welded is gas tungsten arc welding (GTAW). In this welding process, the shielding gas used has physical properties, such as density, thermal and electrical conductivity, and ionization potential, among others, capable of affecting the operational characteristics of welding arcs. Characteristics such as welding voltage, heat input, and thermal profile, which affect the geometry (shape, width, and penetration) of welds, are strongly influenced by the properties of the gas used (Refs. 3, 4).

However, despite several studies of the gases used in welding processes, there are still phenomena that are poorly or not researched; for example, the study of the use of preheated shielding gas. Thus, the adjustment of this new variable can provide one more possibility of manipulating the electric arc of the process and, consequently, obtaining welds with different characteristics from those presented in the conventional process.

Thus, this work aimed to evaluate the influence of preheating the shielding gas during the GTAW process on the characteristics of the electric arc, such as welding voltage, profile, and luminosity, and on the geometry of the welds.

From the results obtained in this work, it was observed, from an application point of view, that knowledge of the effects of preheating the shielding gas can be of great value in cases that require low thermal input and a stable electric arc; for example, in micro GTA and thin plate welding.

Experimental Procedures

To heat the gas, an electric resistance system was developed that allowed the maintenance and low changes of its temperature (maximum variation between tests of ± 5°C) during all tests. The gas temperature was monitored at the exit of the welding torch nozzle directly in the gas flow before the arc was opened, without contact or interference from any other part of the torch, using a Minipa Model MT-455 digital

https://doi.org/10.29391/2024.103.026

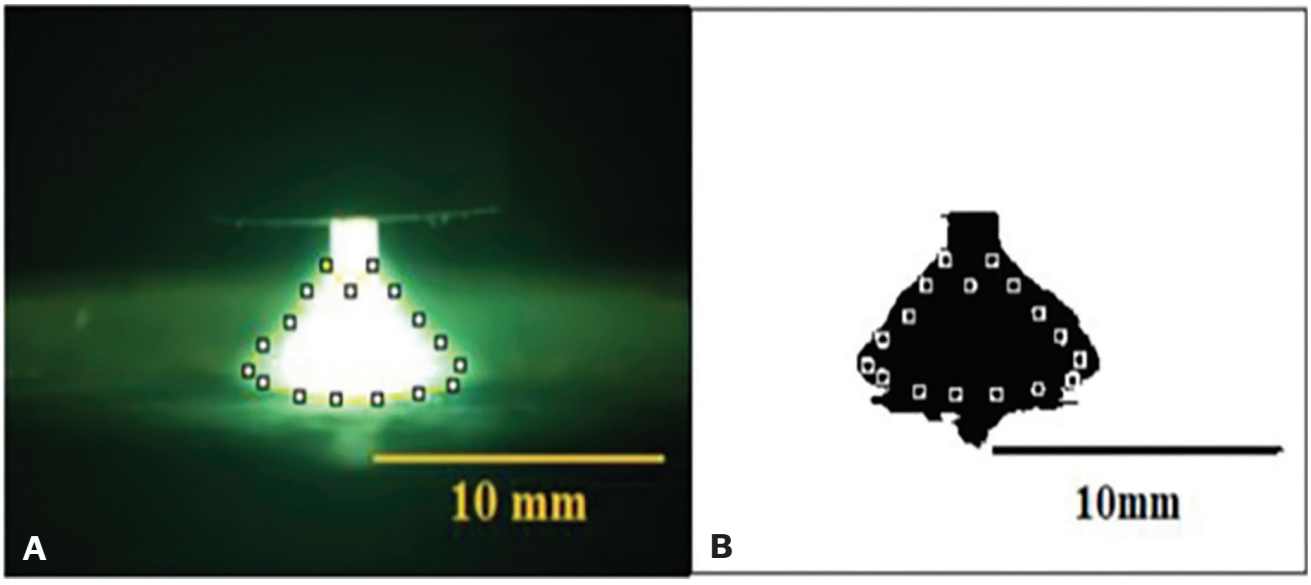

Fig. 1 — Schematic for measuring the arc area using ImageJ software: A — Point-by-point methodology; B — threshold.

Table 1 — Conditions Used to Acquire the Characteristic Curves of the GTAW Electric Arc

Arc Length	Electrode		
	Sharpening Angle	Diameter	Type
4 mm	60 deg	1.6 mm	EWP
Nozzle	Shielding Gas		
	Temperature		Flow
No. 4	Ambient	150°C	6 L/min
Nominal Current (A)			
10	20	30	40
50	60	70	80
90	100	110	120
130	140	150	

thermometer and Type K thermocouple with a precision of ± 0.75% in reading. This temperature monitoring was performed before performing all the experiments proposed in this work and repeated at the end of each analysis.

An argon gas heating temperature of 150°C was limited by the available materials for the assembly of the GTAW torch and the heater.

The study of the electric arc was performed on a cooled copper block without the production of a fusion puddle. Measurements of the operating voltage-current values, arc profile, and emitted brightness were made for the gas with and without heating.

Autogenous welding was performed on ASTM A36 carbon steel plates to determine the penetration and width of the gas at different temperatures.

Aware that the electrodes with oxide addition provide a reduction in their consumption and an improvement in the opening and stability of the electric arc (Ref. 1), pure tungsten electrodes (EWP) were used because they allowed a better observation of the occurrence of significant variations in these factors when the gas was heated.

Study of the Electric Arc

In this study, the same positioning of the welding torch was used for the measurement of the voltage-current values, arc images, and brightness. In all cases, the arc striking was performed by touch, the gas flow rate was measured with a bibimeter, and the electrode sharpening angle was checked with the aid of a goniometer. These procedures were repeated every time before starting the next analysis.

The arc was allowed to stabilize for approximately 5 s after it was initiated before acquiring the values of current, voltage, arc images, and luminosity. These values were then acquired in 10 s.

For the acquisition of welding data, a system from IMC Welding, Model SAP V4, was used together with the software SapTiV4.37s from the same manufacturer.

In Table 1, the conditions employed are defined by the best results presented in the welds produced in this work.

One of the objectives of the acquisition of the voltage-current curve was to reproduce the characteristic curve

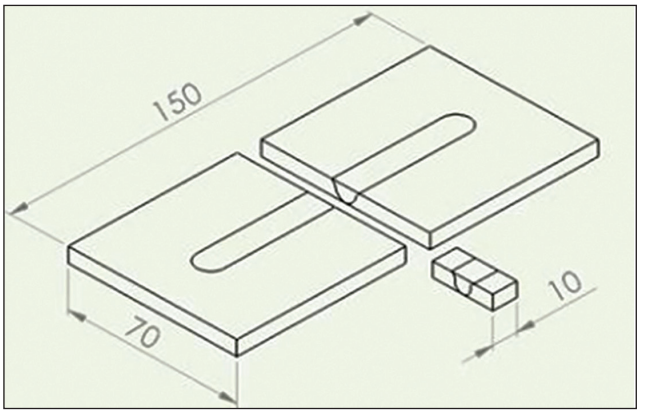

Fig. 2 — Position for taking samples from the welds to perform the characterizations.

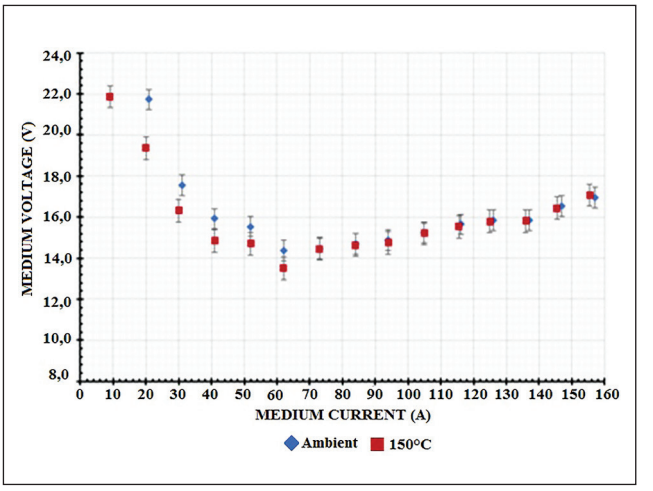

Fig. 3 — GTAW arc characteristic curve for gas at different temperatures.

Table 2 — Welding Parameters Used

Arc Length	Electrode		
	Sharpening Angle	Diameter	Type
4 mm	60 deg	1.6 mm	EWP
Nozzle	Shielding Gas		
	Temperature		Flow
No. 4	Ambient	150°C	6 L/min
Nominal Current (A)			
80	90	100	110
120		130	

presented in the literature (Ref. 5), but the variable in this work was the gas exit temperature and not the arc length.

The voltage acquisition procedure was initiated with a current of 150 A, and the subsequent ones were in intervals of 10 A until the final value of 10 A. The operating current adopted at the beginning of each test was considered the one presented in the welding source sensor (nominal current), but the one used for determining the results was the one obtained by the data acquisition system (measured current).

Arc profiles were observed using a Canon I3 camera placed on a dedicated tripod, which caused the same positioning for the acquisition of all images (30 cm in relation to the cooling block where the arc was opened). Image acquisition followed the care presented in the literature and expressed by Vilarinho (Ref. 6), such as the same positioning of the camera for image acquisition and the use of a light filter for the Level 14 welding mask for protection against the luminosity generated by the arc.

The images obtained were transferred to the free software ImageJ to measure the arc area and relate the results to the different gas temperatures. The methodology for measuring these areas followed the delimitation of the arc region point by point (Fig. 1), with the software providing the area values. Along with this methodology, the threshold procedure of the same software was also used to compare the values and reduce measurement errors (the region to be analyzed is defined, and the regions of different colors are separated into black and white scales).

For each current, three image acquisitions were performed, their areas were measured, an average of the obtained values was taken, and measurement errors were evaluated.

To perform this experiment, a Minipa Model MLM-1020 digital lux meter was used. The device was accompanied

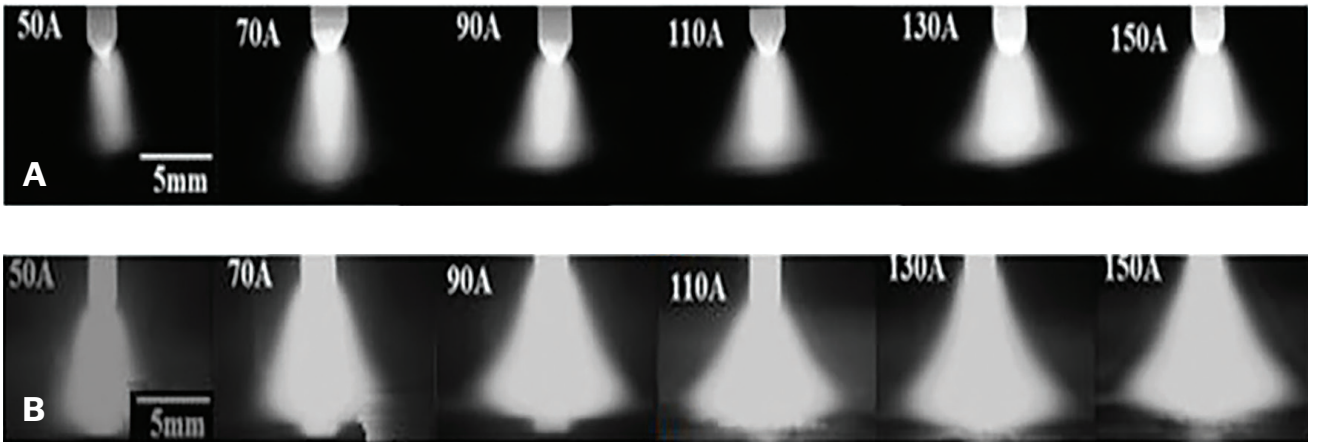

Fig. 4 — Images of the electric arc in relation to the high currents and gas heating temperature: A — Ambient; B — 150°C.

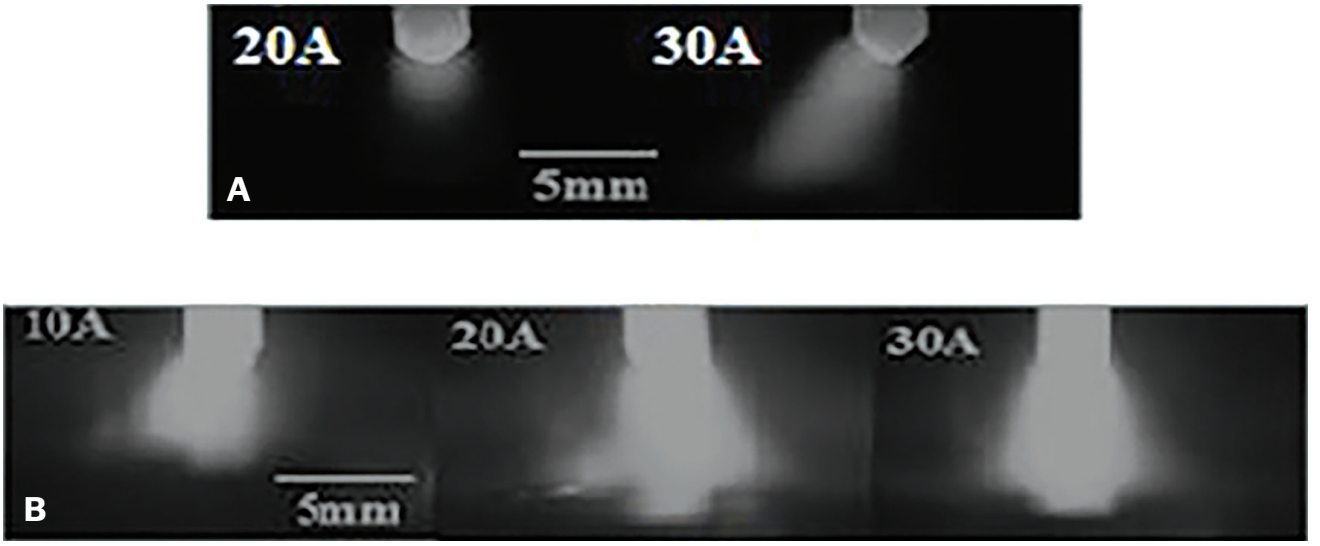

Fig. 5 — Images of the arc for the lowest currents. Temperature of the shielding gas: A — Ambient; B — 150°C.

by the software responsible for data acquisition; the values obtained were represented in the lux unit, and the acquisition interval was one point every second. The relative precision of the acquisition was ± 0.75% on the reading; that is, ± 3%, according to the data provided by the manufacturer.

The lux meter was positioned at a fixed distance from the electric arc (6 cm) and protected by a light filter for the Level 6 welding mask. To obtain an average of the luminosity values obtained, three tests were performed for each current established.

Before each test, the electrode was sharpened, and it was observed whether the initial luminosity shown in the device was zero (aiming to evaluate only the luminosity produced by the electric arc and no other external light source present during the tests).

Welding

This study evaluated the effect of heating gas on the geometry of the welds produced. To do so, welds were performed on ASTM A36 steel plates with the GTAW process without the addition of material. The welding torch was kept fixed while moving the test plate, which provided the same torch positioning in relation to the plates during all of the welds. The welding speed was kept constant using a mechanized displacement-controlled device.

Along with the welds, voltage and current were monitored with the aid of the data acquisition system previously presented in the arc study.

The test plates had dimensions of 150 × 70 × 6.35 mm (length, width, and thickness), and they were cleaned before the tests using abrasive blasting and afterward using the flap-type grinding disc.

To produce the welds, some of the parameters were kept constant to evaluate the effect of gas temperature at dif-

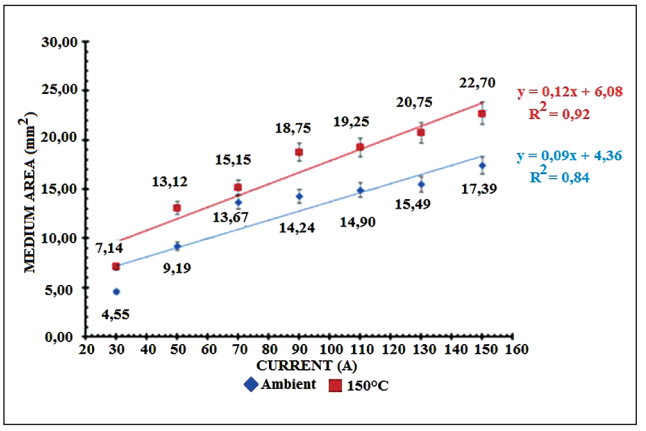

Fig. 6 — Arc area measured by ImageJ software as a function of current and gas heating temperature.

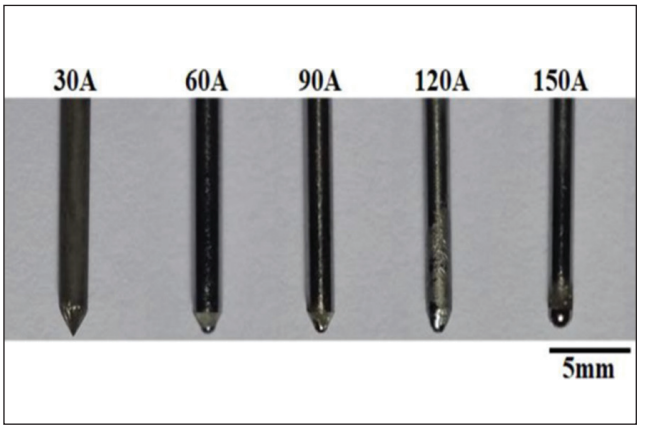

Fig. 7 — Electrodes after performing tests with the heated gas.

Table 3 — Energy Contribution Provided by the Heating of the Shielding Gas

I (A)	U (V)	P (W)	P_{Gas}/P_{Arc} (%)
10	~22	220	4.1
30	~17	510	1.8
50	~15	750	1.2
70	~15	1050	0.9
90	~15	1350	0.7
110	~15	1650	0.6
130	~16	2080	0.5
150	~16	2400	0.4

ferent operating currents. These parameters are presented in Table 2.

For each of the welding currents, three welds were made, which generated a total of 36 samples. The arc opening was maintained by touch.

To maintain the same parameters as those used in the study of the electric arc, welding was carried out while keeping the parameters constant, as shown in Table 2. However, at welding currents below 80 A, the formation of a weld puddle did not occur, making analysis impossible.

The characterizations of the welds were done by macrostructure analysis, observing changes in the geometry of the welds (width and penetration).

The samples for the macrostructure analysis (penetration and width) were taken from the GTA welds in the central region of the weld beads, as indicated in Fig. 2. For the preparation of these samples, the standard metallography procedure for carbon steel welds was followed; that is, embedding cut, sanding (with 80, 220, 400, and 600 mesh sandpaper), and chemical attack with 5% Nital. Then the cross-section of these welds was photographed with a Canon I3 digital camera, and a ruler was used as a scale.

The photographed images of the welds were taken to the public domain software ImageJ, where a scale bar was introduced and the penetration, width, and area values of the welds were measured. The latter measurement was made using the point-by-point weld region delineation methodology, like the procedure used in the arc area measurement discussed in the previous section.

Results

To understand the effects of heating the shielding gas used in the GTAW process, studies were carried out on the behavior of variables in relation to the change in gas temperature. Among them were the ionization of the electric arc, voltage, current, energy contribution, area of the electric

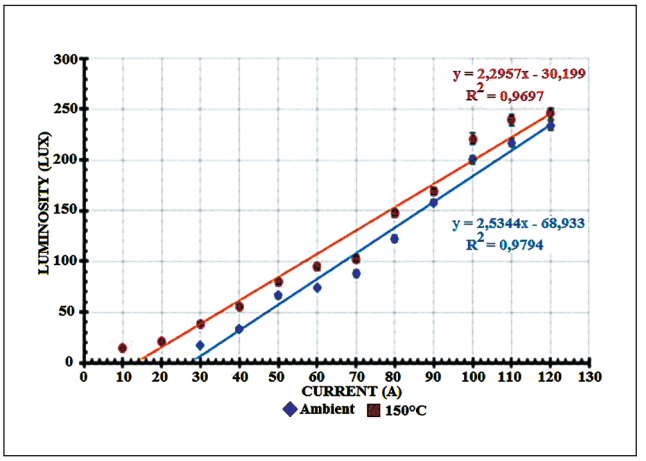

Fig. 8 — Arc luminosity as a function of the current of gas without and with heating.

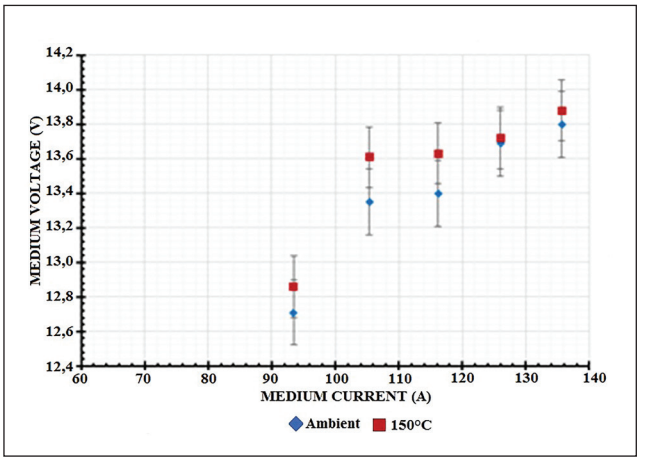

Fig. 9 — Measured voltage and current values for the welds.

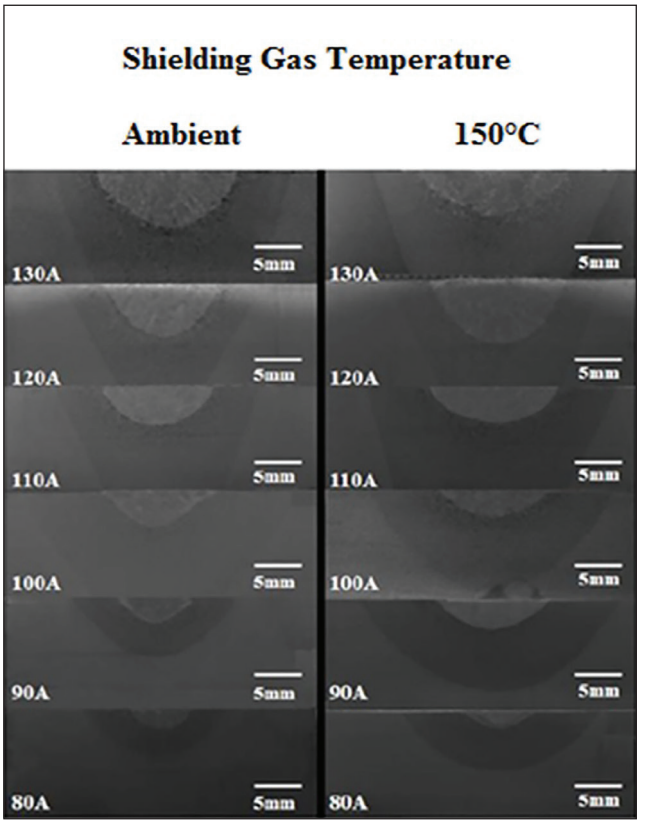

Fig. 10 — Weld macrostructures for different shielding gas temperatures.

arc, current density, effect on the electrode, arc luminosity, and weld geometry.

Study of the Electric Arc

The degree of ionization was calculated by evaluating only the gas heating temperature (150°C or 423K). To do so, the Saha Equation was used for the single ionization of argon, observing only the contribution of the temperature variation of the shielding gas to the value of the degree of ionization (Ref. 1).

$$\frac{\alpha^2}{1-\alpha^2} p/p_0 = 1{,}264 \cdot 10^{-6} T^{5/2} \left(2 + e^{-2062/T}\right) \cdot e^{-183 \cdot 10^3/T} \quad (1)$$

where α represents the degree of ionization, p is the gas pressure, p_0 is the atmospheric pressure, T is the gas temperature, and e is the electron charge ($1.602 \cdot 10^{-19}$C).

When the calculations were performed, the value $1.043 \cdot 10^{-158}$ was obtained, which represents a very low value, but when compared to the unheated gas ($4.74 \cdot 10^{-256}$), the gain in the degree of ionization when the welding process was performed by heating the gas to 150°C was approximately $2.2 \cdot 10^{180}$%.

This increase in the degree of ionization value when heating the shielding gas influenced the ionization and electrical conductivity of the arc column as more electrons were available. This shows that even on a small scale, heating the shielding gas influences the electrical properties.

Then the values for the arc voltage and current were obtained, as presented in the graph in Fig. 3. It is noteworthy that there are no voltage values for the current of 10 A due to not opening the arc in the test in which the shielding gas was not heated.

It can be seen in the graph of Fig. 3 that the measured voltage values presented a decrease in the difference in their values with the shielding gas without and with heating (ambient and normal) for the current range of 10 to 70 A. For the larger currents (80 to 150 A), the voltage values were similar, which represents a reduction in the influence of the gas heating on voltage values with the increase in operating current.

The curve shown in Fig. 3 reproduces the behavior of characteristic curves found in the literature (Ref. 5), highlighting, as shown in this work, the parameterization variable, which was the temperature of the shielding gas.

These voltage variations, observed in Fig. 3, for the smaller currents (10 to 70 A), had a greater effect on the column of the arc. In a model for analyzing the effects of arc current

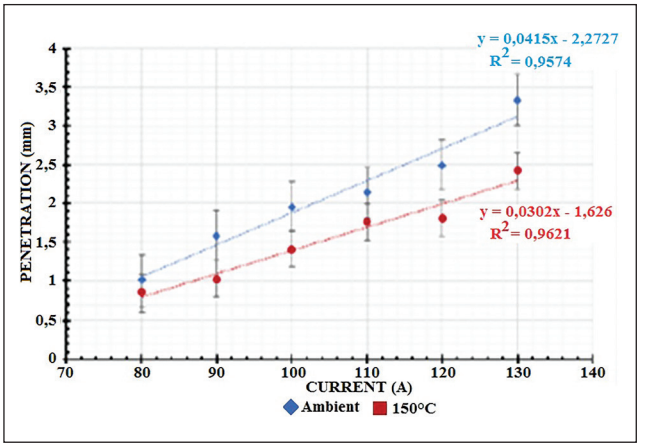

Fig. 11 — Weld penetration for different shielding gas temperatures.

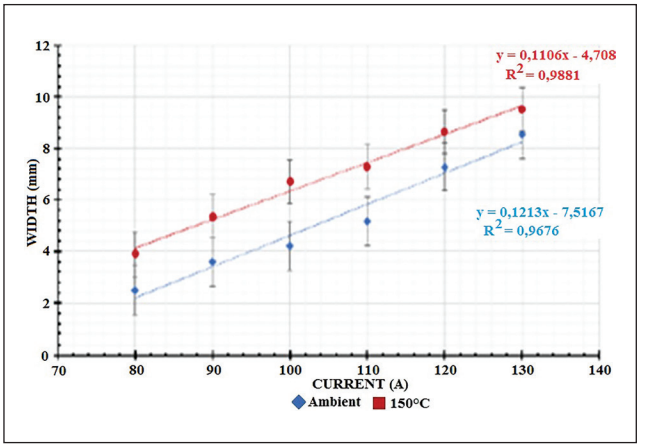

Fig. 12 — Weld width for different shielding gas temperatures.

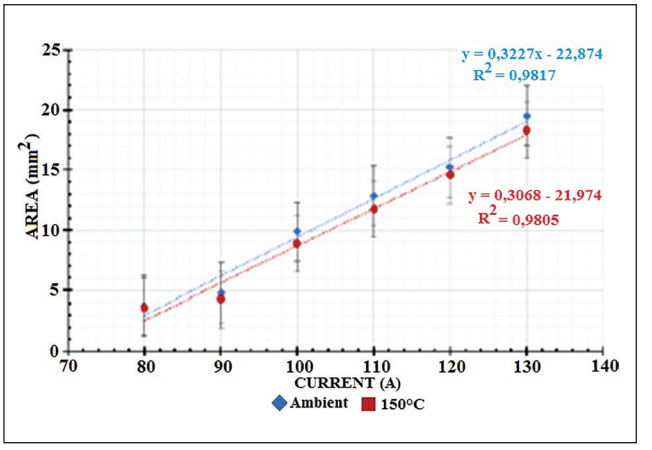

Fig. 13 — Weld area for different shielding gas temperatures.

and voltage, Lancaster (Ref. 1) attributes that the welding current has a direct relationship with the amount of heat transferred to the workpiece and is, therefore, a key variable in determining the amount of fusion in the base metal and weld penetration. On the other hand, voltage has a smaller effect on penetration because its variations cause greater effects on the arc column, whose generated heat is transmitted mainly in the radial direction. It is noteworthy that arc length is directly associated with its voltage and the welding arc has a truncated cone shape, so it can be concluded that welding voltage affects, above all, weld width.

The reduction in the effect of shielding gas heating on voltage values was calculated and determined from the current range used. These are presented in Table 3.

Considering the 100% efficient welding process, the power supplied by the electric arc was considered by the relationship between the voltage and the welding current; that is, $P_{arc} = U \cdot I$ (where P_{arc} or P is the power of the arc, U is the voltage, and I is the current).

To arrive at the P_{gas}/P_{arc} relationship, the power value of the contribution provided by heating the shielding gas was calculated using the thermodynamic power equation:

$$P_{Gas} = \frac{Q}{\Delta t} \rightarrow Q = mc\Delta T \qquad (2)$$

where P_{gas} is the power supplied by heating the gas, Q is the heat, Δt is the time variation, m is the mass of gas, c is the specific heat, and ΔT is the temperature variation. In this way, a value of 9.8W was obtained for the power supplied only by the heating effect of the shielding gas.

The values observed in Table 3 reinforce the idea of a reduction in the contribution of gas heating to the voltage values as the operating current increased.

For the low-current region (I < 70 A), the voltage decreased with increasing current. This can be explained by the fact that increasing the electric current incurs greater heating of the cathode (facilitating the emission of electrons) and a greater degree of ionization and heating of the medium in which the arc occurs, resulting in greater ease for the passage of current and, consequently, a decrease in electric arc voltage (Refs. 2, 7, 8). As observed in Table 3, the greater effect of heating the shielding gas at lower currents influenced the conditions discussed (electron emission, degree of ionization, and electrical conductivity), resulting in a decrease in the voltage values in the region between 10 and 70 A until similar values for the high currents (80 to 150 A), in which the contribution of heating the gas was lower.

Images of the electric arc were acquired together with the acquisition of the results presented above. Each image was related to the nominal operating current used and the gas heating temperature. With these images, arc area measurements were taken, and the main differences were evaluated.

Figures 4 and 5 represent the images of the arc for the higher and lower currents, respectively, as a function of shielding gas temperature.

Analyzing the images of the electric arc, it was possible to observe an increase in the area for all currents determined when heating the shielding gas. The greatest differences were found in the smallest currents (10 to 30 A), highlighting the near extinction of the electric arc and the formation of punctual anodes in the case where the gas was not heated.

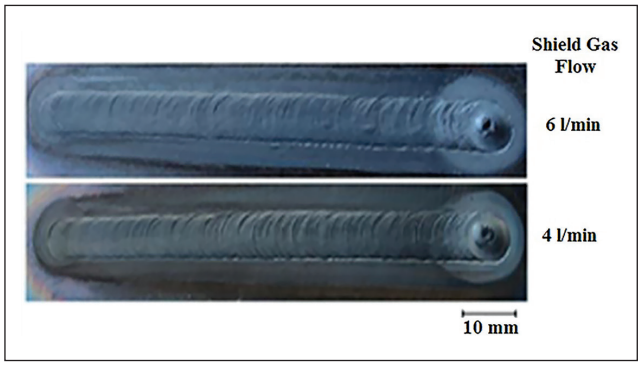

Fig. 14 — Images of weld surfaces with different flow rates of shielding gas heated to 150°C.

The values of the electric arc areas as a function of the currents are shown in the graph in Fig. 6, highlighting the values that were always higher when the shielding gas was heated. A reduction in the difference between the measured values of the arc area was observed for the shielding gas without and with heating when decreasing the operating current.

According to the images of the arc shown in Figs. 4 and 5, greater heating of the electrode was observed when using heated gas; this effect influenced the cathodic fall and emission of electrons. Thus, the empirical Richardson-Dushman Equation (Equation 3, Refs. 2, 9) was used to determine the current density value when the shielding gas was heated, using the electrode temperature value of 150°C and comparing it with the same at room temperature (25°C). This calculation was performed to evaluate the effect of the heated gas in contact with the tungsten electrode during welding and compare it with the conventional process with the gas at room temperature.

$$J = AT^2 \exp\left(\frac{-e\phi}{kT}\right) \quad (3)$$

where J is the current density, A is the thermionic constant ($7.0 \cdot 10^5$ A/m^2), and ϕ is the work function of the material.

The current density value only related to the heating of the shielding gas was $JW = 1.60 \cdot 10^{-57}$ A/m^2 (25°C) and $JW = 3.04 \cdot 10^{-37}$ A/m^2 (150°C), representing an improvement of $1.9 \cdot 10^{22}$% only in relation to the effect generated by heating the gas.

Thus, the arc expansion observed in Figs. 4 and 5 was related to the effects generated by the heating of the shielding gas in the arc column, such as the variation in the degree of ionization, electrical conductivity, and current density. Even at a temperature far below that of the electric arc, heating the shielding gas influenced the degree of ionization, electrical conductivity, and current density when compared to the values obtained from the gas at room temperature, as calculated.

Heating the shielding gas improved the emission of electrons but reduced the life of the electrode, accelerating the loss of its sharpness. This deterioration of the electrodes was related to their increased heating by the passage of the shielding gas at 150°C. Figure 7 shows the electrodes used in this work for currents between 30 and 150 A and a test time of 15 s.

It can be seen in Fig. 7 that for lower currents, the electrodes presented lower consumption; for example, for the currents of 30 and 60 A. When the current was increased, consumption increased, even losing sharpening completely, as in the case of the 150 A current. It was found that without heating the protective gas, the electrodes presented very little wear since maintenance of the original sharpening was observed after the tests for all currents used.

The change in the arc profile (increase of its area) influenced the results obtained for its luminosity (arc expansion implied a larger area of light emission), influence in the thermal yield (higher thermal losses occurred in the arc column), and influence in the welds (changes in weld morphology).

Figure 8 shows the graph of luminosity obtained as a function of current for the two shielding gas temperatures. The luminosity values for the current below 30 A for the unheated gas were not measured due to the instability and non-opening of the arc.

Considering only the gas heating temperature (150°C), in the emissivity of radiation through the arc surface, defined by the Stefan-Boltzmann Law, in which the Stefan-Boltzmann constant has the value of ($5.67 \cdot 10^{-8}$ Wm^{-2}K^{-4}), a light emission of approximately $\varepsilon = 447.15$ Wm^{-2} (25°C) and $\varepsilon = 1815.28$ Wm^{-2} (150°C) was observed, which represented an increase of approximately 25% in the radiation emission of the arc, justifying the results observed in the graph in Fig. 8.

Weld Analysis

As defined in the previous "Welding" section , the welding results were designated with a minimum current of 80 A, as below this value no welding pool formation occurred using the same parameters applied in electric arc studies.

The voltage values for the currents determined in the analysis of the welds were monitored (Fig. 9), and similarity was observed for the different gas temperatures (ambient and 150°C). This behavior was also observed previously when analyzing the effects of heating the shielding gas on the arc for higher current ranges. However, unlike the procedure adopted in the study of the arc, in which the anode was cooled (without the formation of a fusion pool) in the welds, there was a greater generation of metallic fumes. Despite the small number of metallic vapors near the fusion puddle, several studies (Refs. 10–18) demonstrated that they altered the physical properties of the arc. Among the changes, the one that stands out most is the increase in electrical conduction and that of radiation (electromagnetic emissivity).

The increase in radiation implies more energy being sent out of the electric arc, which causes the temperature of the arc regions affected by the metal vapors to decrease. Gonzalez and coworkers (Ref. 19) presented in their work that iron vapors in the arc at a concentration of approximately 0.1% can cause a 1000K decrease in arc temperature, and Razafinimanana and coworkers (Ref. 13) obtained a 2000K decrease in arc temperature when the vapors were copper at a concentration of 1%.

Rossi and coworkers (Ref. 20) demonstrated in their work that the metallic vapors generated in chilled copper blocks (like the one used in this work for the arc analysis, voltage-current curves in the "Study of the Electric Arc" section) change the arc's behavior, such as the generation of arc coupling points at the anode. This author attributes this same behavior when making welds in steel plates, differentiating with the copper anode, to the greater generation of metallic vapors produced by the steel melting, influencing the voltage and thermal emissivity values.

The macrostructure of the welds was observed, and Fig. 10 shows these macrostructures as a function of the nominal currents determined and the temperatures of the shielding gas. Figure 10 shows a reduction in the penetration and an increase in the width of the welds when the gas was heated.

The results presented in Fig. 10 are directly linked to what was observed in the study carried out for the electric arc when its profile was analyzed; that is, the occurrence of the arc expansion when the gas was heated.

The values of penetration, width, and area of the welds were measured from the macros as described in the methodology and plotted in the graphs in Figs. 11–13, respectively. By analyzing these figures, it was observed that the difference between the two shielding gas temperatures in the penetration and width values varied with the increase of current, and the weld area presented small modifications.

One explanation for the effects observed in the welds with heated gas was the expansion of the arc, a fact that facilitated the passage of the arc into the puddle in the regions where its temperature was lower, resulting in greater width in the welds. This changed the dimensions of the anodic spot, which were increased; the heating acted as a facilitator to the electrical movement of the arc (increasing the electrical conductivity in the arc column, calculated previously by Equation 2). This expansion of the electric arc caused the penetration to decrease due to the energy distribution of the column in a larger area. Some authors (Ref. 21) conducted studies evaluating this interaction between the characteristics of the arc and the fusion puddle with the use of argon as a shielding gas and the DC process.

Another qualitative test performed on the welds was the reduction of the gas flow rate from 6 l/min to 4 l/min, keeping all other parameters constant. In this test, it was observed that heating the shielding gas allowed reduction of flow without changing the weld. This occurrence can be confirmed by Fig. 14, which shows images of the surface of two welds made with a current of 100 A, the gas at 150°C, and flow rates of 6 l/min and 4 l/min, respectively.

The behavior shown in Fig. 14 was not possible without heating the shielding gas (i.e., at room temperature, there was a lack of protection when using the flow rate of 4 l/min, not producing welds with similar aspects).

Despite the reduction of the shielding gas flow rate (4 l/min) and its heating (150°C), the flow remained laminar, as observed when calculating the Reynolds number (Re) for the 100A arc as being approximately 350 (w = 2.1 m/s; p = 0.774 kg/m3; d = 2.97•10-5 kg/ms), where w is the velocity, p is the density, and d is the dynamic viscosity of the plasma. McKelliget and Szekely (Ref. 22) and Wendelstorf and coworkers (Ref. 23) state that the transition from the laminar-turbulent regime happens in the GTAW arc for values of Re above 500. This may be one of the reasons for the lack of protection when using a shielding gas flow rate of 4 l/min with the gas without heating, due to the more turbulent flow (Re ~ 524).

Conclusions

In function of the objective proposed in this work (that is, to evaluate the influence of the temperature of the shielding gas used in the GTAW process), the following conclusions were reached:

- The changes due to the use of heated shielding gas mostly applied to welding currents of 10 to 70 A.
- Heating the shielding gas influenced the degree of ionization, current density, and electrical conductivity of the arc column. These changes caused an expansion of the arc and increased light emission, giving welds lower penetration and greater width. These factors can be beneficial in welds that require greater control of the heat input, such as thin plate welds.
- It was observed that heating the gas allowed the use of low currents (10–70 A), even with a large arc length (4 mm), and this effect is applied in welds that require low currents and arc stability, as in micro GTA welding.
- In initial tests, it was possible to reduce the flow of the shielding gas when heating it, which suggests a reduction in its consumption and a lower process cost.

Thus, heating the shielding gas used in the GTAW process was beneficial in welds that required greater control of heat input and in lower current ranges (10–70 A) and provided a reduction in the consumption of shielding gas.

References

1. Lancaster, J. F. 1986. *The Physics of Welding*. Pergamon Press & International Institute of Welding. DOI: 10.1016/C2013-0-03805-4

2. Guile, A. E. 1971. Arc-electrode phenomena. *Proceedings of the Institution of Electrical Engineers Reviews* 118(9R). DOI: 10.1049/piee.1971.0246

3. Dwivedi, D. K. 2021. Physics of welding arc. *Fundamentals of Metal Joining*. DOI: 10.1007/978-981-16-4819-9_6

4. Singh, B., Singhal, P., and Kumar Saxena, K. 2019. Investigation of thermal efficiency and depth of penetration during GTAW process. *Materials Today: Proceedings* 18(7): 2962–2969. DOI: 10.1016/j.matpr.2019.07.166

5. Marques, P. V., and Modenesi, P. J. 2015. Some handy equations for welding. *Soldagem & Inspeção* 19(1): 091–102. DOI: 10.1590/S0104-92242014000100011

6. Vilarinho, L. O., Lucas, B., and Raghunathan, S. S. 2009. Issues before performing measurements from pictures/films in welding. *Soldagem & Inspeção* 14(4). DOI: 10.1590/S0104-92242009000400011

7. Khoshnaw, F., Krivtsun, I., and Korzhyk, V. 2023. Chapter 2 – Arc welding methods. *Welding of Metallic Materials*, 37-71. DOI: 10.1016/B978-0-323-90552-7.00004-3

8. Xie, W., Zhou, Y., and Nian, K., et al. 2023. Effect of process parameters on arc behavior and weld formation in weaving gas tungsten arc welding. *Materials Engineering and Performance*. DOI: 10.1007/s11665-023-07913-6

9. Richardson, O. W. 1929. *Thermionic phenomena and the laws which govern them*. Nobel Lecture.

10. Cressault, Y., et al. 2008. Influence of metallic vapours on the properties of air thermal plasma. *Iopscience: Plasma Sources Science and Technology* 17(13) 1–9. DOI: 10.1088/0963-0252/17/3/035016

11. Cheminat, B., and Andanson, P. 1985. Conduction in an electric arc column contaminated by copper vapour. *Iopscience: Journal of Physics D: Applied Physics* 18(11): 2183–2192. DOI: 10.1088/0022-3727/18/11/008

12. Vacquie, S. 1996. Influence of metal vapours on arc properties. *Pure and Applied Chemistry* 68(5): 1133–1136. DOI: 10.1351/pac199668051133

13. Razafinimanana, M., et al. 1995. Experimental study of the influence of anode ablation on the characteristic of an argon transferred arc. *Iopscience: Plasma Sources Science and Technology* 4(3): 501-510. DOI: 1088/0963-0252/4/3/021

14. Murphy, A. B., et al. 2009. Modelling of thermal plasma for arc welding: the role of the shielding gas properties and of metal vapour. Iopscience: *Journal of Physics D: Applied Physics* 42(19): 1-20. DOI: 10.1088/0022-3727/42/19/194006

15. Schnick, M., et al. 2010. Metal vapour causes a central minimum in arc temperature in gas-metal arc welding through increased radiative emission. *Iopscience: Journal of Physics D: Applied Physics* 43(2): 1-5. DOI: 10.1088/0022-3727/43/2/022001

16. de Simas Asquel, G., Bittencourt, A.P.S., and Vieira da Cunha, T. 2020. T.V. Effect of welding variables on GTAW arc stagnation pressure. *Welding in the World* 64: 1149–1160. DOI: 10.1007/s40194-020-00919-x

17. Fan, D., Zhang, R., Gu, Y., and Ushio, M. 2001. Effect of flux on A-TIG welding of mild steels. *Transactions of Joining and Welding Research Institute* 30(1): 35–40.

18. Murphy, A. B. 2010. The effects of metal vapour in arc welding. *Journal of Physics D: Applied Physics* 43(43). DOI: 10.1088/0022-3727/43/43/434001

19. Gonzalez, J. J., Bouaziz, M., Razafinimanana, M., and Gleizes, A. 1997. The influence or iron vapour on an argon transferred arc. *Plasma Sources Science and Technology* 6(1): 20–28. DOI: 10.1088/0963-0252/6/1/004

20. Rossi, M. L., Ponomarev, V., and Scotti, A. 2016. Heat exchange and voltage drop in welding arc column. *IEEE Transactions on Plasma Science*: 1–9. DOI: 10.1109/TPS.2016.2606628

21. Delgado-Álvarez, A., Mendez, P. F., and Ramírez-Argáez, M. A. 2019. Dimensionless representation of the column characteristics and weld pool interactions for a dc argon arc. *Science and Technology of Welding and Joining* 24(7): 634–643. DOI: 10.1080/13621718.2019.1584455

22. McKelliget, J., and Szekely, J. 1986. Heat transfer and fluid flow in the welding arc. *Metallurgical Transactions A* 17: 1139–1148. DOI: 10.1007/BF02665312

23. Wendelstorf, J., et al. 1996. TIG and plasma arc modelling: A survey, in mathematical modelling of weld phenomena 3. *The Institute of Materials*: 848–89.

NILO NOGUEIRA DA SILVA (*nilons.fisica@gmail.com*) is with the Innovation and Technology Center (CIT-SENAI) – Institute of Innovation in Metallurgy and Special Alloys (ISI MLE), Minas Gerais, Brazil. **WAGNER SADE** is with the Federal Center for Technological Education of Minas Gerais (CEFET-MG) – Mechanical Engineering Department, Minas Gerais, Brazil.